

spAbundance: An R package for single-species and multi-species spatially-explicit abundance models

Jeffrey W. Doser^{1, 2}, Andrew O. Finley^{2, 3, 4}, Marc Kéry⁵, Elise F. Zipkin^{1, 2}

¹Department of Integrative Biology, Michigan State University, East Lansing, MI, USA

²Ecology, Evolution, and Behavior Program, Michigan State University, East Lansing, MI, USA

³Department of Forestry, Michigan State University, East Lansing, MI, USA

⁴Department of Statistics and Probability, Michigan State University, East Lansing, MI, USA

⁵Swiss Ornithological Institute, Sempach, Switzerland

Corresponding Author: Jeffrey W. Doser, email: doserjef@msu.edu; ORCID ID: 0000-0002-8950-9895

Abstract

1. Numerous modeling techniques exist to estimate abundance of plant and wildlife species. These methods seek to estimate abundance while accounting for multiple complexities found in ecological data, such as observational biases, spatial autocorrelation, and species correlations. There is, however, a lack of user-friendly and computationally efficient software to implement the various models, particularly for large data sets.
2. We developed the **spAbundance** R package for fitting spatially-explicit Bayesian single-species and multi-species hierarchical distance sampling models, N-mixture models, and generalized linear mixed models. The models within the package can account for spatial autocorrelation using Nearest Neighbor Gaussian Processes and accommodate species correlations in multi-species models using a latent factor ap-

proach, which enables model fitting for data sets with large numbers of sites and/or species.

3. We provide three vignettes and three case studies that highlight **spAbundance** functionality. We used spatially-explicit multi-species distance sampling models to estimate density of 16 bird species in Florida, USA, an N-mixture model to estimate Black-throated Blue Warbler (*Setophaga caerulescens*) abundance in New Hampshire, USA, and a spatial linear mixed model to estimate forest aboveground biomass across the continental USA.
4. **spAbundance** provides a user-friendly, formula-based interface to fit a variety of univariate and multivariate spatially-explicit abundance models. The package serves as a useful tool for ecologists and conservation practitioners to generate improved inference and predictions on the spatial drivers of populations and communities.

1 Introduction

Understanding how abundance of plant and animal populations varies across space and time is a central objective in ecology and conservation management. A variety of sampling and associated modeling techniques have been developed over the last 50 years to estimate abundance while accounting for imperfect detection (i.e., the failure to observe all individuals of a species that are present at a location during the sampling period), including distance sampling and repeated counts, among others (Nichols et al., 2009). In distance sampling, the probability of detecting an individual is assumed to decay with increasing distance to the observer, which allows for the explicit estimation of abundance/density while accommodating imperfect detection of individuals (Buckland et al., 2001). Hierarchical distance sampling (HDS; Royle et al. 2004) extends classical distance sampling to enable modeling abundance/density as a function of spatially-varying covariates. Royle et al. (2004) introduced N-mixture models, which allow for estimation of abundance (and effects of spatially-varying covariates) while accounting for detection probability using replicated count data during some period where the population is assumed to be closed (i.e., no births/deaths or immigration/emigration). In addition to approaches that explicitly account for imperfect detection, generalized linear mixed models (GLMMs) that estimate relative abundance (i.e., ignoring imperfect detection) can be used to assess how environmental covariates influence relative changes in abundance across space and/or time (Barker et al., 2018; Goldstein and de Valpine, 2022). Multi-species (i.e., multivariate) extensions of HDS (Sollmann et al., 2016), N-mixture models (Yamaura et al., 2012), and GLMMs (e.g., Hui et al. 2015) use count data from multiple species to estimate species-specific patterns in abundance, which may also estimate correlations between species in a joint species distribution model (JSDM) framework (Warton et al., 2015).

When modeling abundance across large spatial domains and/or using a large number of observed locations, accommodating spatial autocorrelation becomes increasingly important (Guélat and Kéry, 2018). Spatial autocorrelation can arise from a variety of ecological and/or biological processes, such as additional environmental drivers not

included as covariates in the model, dispersal, species interactions, and source-sink metapopulation dynamics (Chapter 9; [Kéry and Royle 2021](#)). Failing to account for residual spatial autocorrelation (i.e., remaining spatial autocorrelation after accounting for environmental covariates) can lead to overly precise estimates and inferior predictive performance. Modeling spatial dependence is commonly done via the addition of spatially structured random effects to point-referenced spatial regression models (i.e., spatially-explicit models). Gaussian process-based random effects provide a flexible non-parametric approach to capture spatial patterns, offer unparalleled process parameter and predictive inference, and yield probabilistic uncertainty quantification. The hierarchical Bayesian framework is the preferred inferential framework for models developed here and in the literature due to their increased flexibility to fit models that would be infeasible with classical methods ([Banerjee et al., 2014](#)). Such models are, however, notoriously computationally intensive ([Banerjee and Fuentes, 2012](#)), as computational complexity increases in cubic order with the number of spatial locations. These computational bottlenecks make fitting spatially-explicit models impractical for even moderately large data sets using Bayesian software packages such as `Stan` ([Carpenter et al., 2017](#)) and `NIMBLE` ([de Valpine et al., 2017](#)).

Many popular, formula-based R packages exist that can fit various combinations of distance sampling models, N-mixture models, and/or spatially-explicit GLMMs for assessing spatial patterns in abundance (Supplemental Information Table S1). The R package `unmarked` ([Fiske and Chandler, 2011](#)) is commonly used to fit single-species distance sampling and N-mixture models, but cannot accommodate spatial autocorrelation. The `dsm` package ([Miller et al., 2013](#)) can fit spatially-explicit distance sampling models using generalized additive models, the `hSDM` package ([Vieilledent, 2019](#)) can fit spatially-explicit N-mixture models with an intrinsic conditional autoregressive model ([Ver Hoef et al., 2018](#)), while the `ubms` package ([Kellner et al., 2021](#)) fits both spatially-explicit distance sampling and N-mixture models using restricted spatial regression ([Hodges and Reich, 2010](#)). These packages, however, cannot accommodate multiple species within a multivariate framework. A variety of R packages exist to fit spatially-explicit univariate

and multivariate GLMMs, such as `spBayes` (Finley et al., 2015), `Hmsc` (Tikhonov et al., 2020), and `sdmTMB` (Anderson et al., 2022). However, none of these packages can explicitly account for imperfect detection.

In this paper, we introduce the `spAbundance` R package for fitting Bayesian single-species and multi-species HDS models, N-mixture models, and GLMMs that may or may not include spatial autocorrelation in large data sets. We fit all spatially-explicit models with Nearest Neighbor Gaussian Processes (NNGPs), a computationally efficient approach that closely approximates a full Gaussian process while drastically reducing computational run times (Datta et al., 2016; Finley et al., 2019). We designed `spAbundance` syntax to closely follow the syntax of `spOccupancy` (Doser et al., 2022), an R package that fits a variety of spatially-explicit occupancy models, which together provide a user-friendly and computationally efficient set of tools to model occupancy and abundance while accounting for spatial autocorrelation and imperfect detection.

2 Overview of models in `spAbundance`

Below we give a brief overview of the models included in `spAbundance`. See Supplemental Information S1 for details on all prior distributions and their default values.

2.1 Single-species hierarchical distance sampling models

The `spAbundance` functions `DS` and `spDS` fit non-spatial and spatial single-species HDS models, respectively. Let $N(\mathbf{s}_j)$ denote the true abundance of a species of interest at site $j = 1, \dots, J$ with spatial coordinates \mathbf{s}_j . We model $N(\mathbf{s}_j)$ using either a Poisson or negative binomial (NB) distribution following

$$\begin{aligned} N(\mathbf{s}_j) &\sim \text{Poisson}(\mu(\mathbf{s}_j)A(\mathbf{s}_j)), \text{ or,} \\ N(\mathbf{s}_j) &\sim \text{NB}(\mu(\mathbf{s}_j)A(\mathbf{s}_j), \kappa), \end{aligned} \tag{1}$$

where $\mu(\mathbf{s}_j)$ is the average abundance at site j , $A(\mathbf{s}_j)$ is an offset, and κ is a positive dispersion parameter. Smaller values of κ indicate overdispersion in the latent abundance

values relative to a Poisson model, while higher values indicate minimal overdispersion in abundance. The offset term $A(\mathbf{s}_j)$ can be used to convert $\mu(\mathbf{s}_j)$ to units of density (i.e., abundance per unit area), while if $A(\mathbf{s}_j) = 1$, $\mu(\mathbf{s}_j)$ is average abundance per site. We model $\mu(\mathbf{s}_j)$ using a log link function following

$$\log(\mu(\mathbf{s}_j)) = \mathbf{x}(\mathbf{s}_j)^\top \boldsymbol{\beta} + \mathbf{w}(\mathbf{s}_j), \quad (2)$$

where $\boldsymbol{\beta}$ is a vector of regression coefficients for a set of covariates $\mathbf{x}(\mathbf{s}_j)$ (including an intercept), $\mathbf{w}(\mathbf{s}_j)$ is a zero-mean spatial random effect, and the \top denotes transposition of column vector $\mathbf{x}(\mathbf{s}_j)$. For non-spatial HDS models, $\mathbf{w}(\mathbf{s}_j)$ is removed from Equation 2. For spatially-explicit HDS, we model $\mathbf{w}(\mathbf{s})$ using a NNGP as a computationally efficient alternative to using a full spatial GP. More specifically, we assume that

$$\mathbf{w}(\mathbf{s}) \sim \text{Normal}(\mathbf{0}, \tilde{\mathbf{C}}(\mathbf{s}, \mathbf{s}', \boldsymbol{\theta})), \quad (3)$$

where $\tilde{\mathbf{C}}(\mathbf{s}, \mathbf{s}', \boldsymbol{\theta})$ is a $J \times J$ NNGP-derived spatial covariance matrix and $\boldsymbol{\theta}$ is a vector of parameters governing the spatial process according to a spatial covariance function. **spAbundance** supports four spatial covariance models: exponential, spherical, Gaussian, and Matérn (Banerjee et al., 2014). For the exponential, spherical, and Gaussian functions, $\boldsymbol{\theta} = \{\sigma^2, \phi\}$, where σ^2 is a spatial variance parameter controlling the magnitude of the spatial random effects and ϕ is a spatial decay parameter controlling the range of spatial autocorrelation, while the Matérn function additionally includes a spatial smoothness parameter, ν . See Supplemental Information S1 for statistical details on the NNGP approximation.

Suppose observers count the number of individuals of the species of interest at each site j . Our software implementation in **spAbundance** supports two types of “sites”: line transects and point count surveys. In line transects, each site j is a line transect the observer walks along and records the distance of each observed individual to the line within a set of $k = 1, \dots, K$ distance bands. In point count surveys, each site j is the center of an imaginary circle at which an observer stands and records the distance of

each observed individual to the center of the circle within $k = 1, \dots, K$ circular distance bands. Note that sometimes continuous distances are recorded rather than distance bins, in which case the continuous distance measurements can then be split into K distance bins prior to analysis. Define $\mathbf{y}(\mathbf{s}_j)$ as a vector of K values indicating the number of individuals observed within each of the k distance bands at site j . Similarly, let $\mathbf{y}^*(\mathbf{s}_j)$ be a vector of $K + 1$ values, where the first K values correspond to $\mathbf{y}(\mathbf{s}_j)$, and the last value is the number of unobserved individuals at that location (i.e., $N(\mathbf{s}_j) - \sum_{k=1}^K y_k(\mathbf{s}_j)$). Note the last value in $\mathbf{y}^*(\mathbf{s}_j)$ is not observed (i.e., since $N(\mathbf{s}_j)$ is not known). We model $\mathbf{y}^*(\mathbf{s}_j)$ according to

$$\mathbf{y}^*(\mathbf{s}_j) \sim \text{Multinomial}(N(\mathbf{s}_j), \boldsymbol{\pi}_j^*), \quad (4)$$

where $\boldsymbol{\pi}_j^*$ is a vector of cell-specific detection probabilities with the first K values denoted as $\boldsymbol{\pi}_j$ and the final value $\pi_{j,K+1} = 1 - \sum_{k=1}^K \pi_{j,k}$. More specifically, $\pi_{j,k}$ is the probability of detecting an individual in the k th distance band at site j . We define $\pi_{j,k}$ as

$$\pi_{j,k} = \bar{p}_{j,k} \psi_k, \quad (5)$$

where $\bar{p}_{j,k}$ is the probability of detecting an individual in distance band k , given the individual occurs in distance band k , and ψ_k is the probability an individual occurs in distance band k . The definitions of $\bar{p}_{j,k}$ and ψ_k are different depending on whether the distance bands are linear (as in line transects) or circular (as in point count surveys). Following the standard distance sampling assumption that animals are uniformly distributed in space, for line transects we have

$$\psi_k = \frac{b_{k+1} - b_k}{B}, \quad (6)$$

where b_{k+1} and b_k are the upper and lower distance limits for band k , and B is the line transect half-width (i.e., the maximum distance within which individuals are counted). Further, for distance x we have

$$\bar{p}_{j,k} = \frac{1}{b_{k+1} - b_k} \int_{b_k}^{b_{k+1}} g(x) dx. \quad (7)$$

For point count surveys, we have

$$\psi_k = \frac{b_{k+1}^2 - b_k^2}{B^2}, \quad (8)$$

where b_{k+1} and b_k are similarly the upper and lower distance limits for band k , and B is the radius of the full point count circle. We then define $\bar{p}_{j,k}$ as

$$\bar{p}_{j,k} = \frac{1}{b_{k+1}^2 - b_k^2} \int_{b_k}^{b_{k+1}} g(x) 2x dx. \quad (9)$$

For both line transects and point count surveys, $g(x)$ is some function of distance x from the transect line/point count survey center. We approximate the integrals in Equation 7 and 9 using numerical integration. Our software implementation in **spAbundance** currently supports two detection functions: half-normal and negative exponential (see Supplemental Information S1 for their definitions). Both of these functions are governed by a scale parameter, σ_j , which can be modeled as a function of covariates to allow detection probability to vary across sites. More specifically, we have

$$\log(\sigma_j) = \mathbf{v}_j^\top \boldsymbol{\alpha}, \quad (10)$$

where $\boldsymbol{\alpha}$ is a vector of regression coefficients for covariates \mathbf{v} (including an intercept).

2.2 Multi-species hierarchical distance sampling models

Now consider the case where distance sampling data, $\mathbf{y}_i(\mathbf{s}_j)$, are collected for multiple species $i = 1, \dots, I$ at each survey location j with coordinates \mathbf{s}_j . We are now interested in estimating the abundance of each species i at each location j , denoted as $N_i(\mathbf{s}_j)$. We model $N_i(\mathbf{s}_j)$ analogous to Equation 1, with expected abundance now varying by species and site according to

$$\log(\mu_i(\mathbf{s}_j)) = \mathbf{x}(\mathbf{s}_j)^\top \boldsymbol{\beta}_i + \mathbf{w}_i^*(\mathbf{s}_j), \quad (11)$$

where $\boldsymbol{\beta}_i$ are the species-specific effects of covariates $\mathbf{x}(\mathbf{s}_j)$ (including an intercept) and $\mathbf{w}_i^*(\mathbf{s}_j)$ is a species-specific random effect. When $N_i(\mathbf{s}_j)$ is modeled using a negative

binomial distribution, we estimate a separate dispersion parameter κ_i for each species. We model β_i as random effects arising from a common, community-level normal distribution, which leads to increased precision of species-specific effects compared to single-species models (Sollmann et al., 2016). For example, the species-specific abundance intercept $\beta_{0,i}$ is modeled according to

$$\beta_{0,i} \sim \text{Normal}(\mu_{\beta_0}, \tau_{\beta_0}^2), \quad (12)$$

where μ_{β_0} is the community-level abundance intercept, and $\tau_{\beta_0}^2$ is the variance of the intercept across all I species. The observation portion of the multi-species distance sampling model is identical to the single-species model and follows Equations 4-10, with all parameters indexed by species, and the species-specific coefficients α_i modeled hierarchically analogous to the species-specific abundance coefficients β_i (Equation 12).

spAbundance fits three types of multi-species models that differ in how they incorporate the species-specific random effect $w_i^*(\mathbf{s}_j)$ (if included). The function **msDS** fits the non-spatial multi-species distance sampling model of Sollmann et al. (2016) in which we remove the random effect $w_i^*(\mathbf{s}_j)$ from Equation 11. The function **sfMsDS** fits spatial multi-species distance sampling models using a spatial factor model (Hogan and Tchernis, 2004), which simultaneously accommodates spatial autocorrelation and residual species correlations in a spatial joint species distribution model framework. Briefly, we decompose $w_i^*(\mathbf{s}_j)$ into a linear combination of q latent variables (i.e., factors) and their associated species-specific coefficients (i.e., factor loadings). More specifically, we have

$$w_i^*(\mathbf{s}_j) = \boldsymbol{\lambda}_i^\top \mathbf{w}(\mathbf{s}_j), \quad (13)$$

where $\boldsymbol{\lambda}_i^\top$ is the i th row of factor loadings from an $I \times q$ loadings matrix $\mathbf{\Lambda}$, and $\mathbf{w}(\mathbf{s}_j)$ is a vector of length q of independent spatial factors at site j . By setting $q \ll I$, we achieve dimension reduction to efficiently model communities with a large number of species (Taylor-Rodriguez et al., 2019; Doser et al., 2023). The approach accounts for residual species correlations via their species-specific responses to the q spatial factors, which results in a residual interspecies covariance matrix that can be derived from the

model as $\Sigma = \Lambda\Lambda^\top$. We model each spatial factor using an independent NNGP according to Equation 3, except we fix the spatial variance parameter to 1 to ensure identifiability (Lopes and West, 2004). As an alternative, the function `lfMsDS` models $w_i^*(\mathbf{s}_j)$ identical to Equation 13, except assumes each of the q factors in $\mathbf{w}(\mathbf{s}_j)$ arises from an independent standard normal distribution. This model does not account for spatial autocorrelation but does allow for the estimation of species correlations. The models fit by `sfMsDS` and `lfMsDS` can be thought of as abundance-based JSDMs that account for imperfect detection (Tobler et al. 2019; Chapter 8 in Kéry and Royle 2021).

Our factor modeling approach to fitting spatially-explicit multi-species models in `spAbundance` implicitly assumes species are correlated through latent factors $\mathbf{w}(\mathbf{s}_j)$. If there is no interest in residual species correlations, we could imagine a multi-species model that includes a separate spatial process for each species. However, we do not include such models in `spAbundance` because they are computationally infeasible when working with even a moderate number of species (e.g., 10). Further, in the context of occupancy models, the spatial factor modeling approach has been shown to perform equally as well as a model that estimates a separate spatial random effect for each species even when there are no residual correlations between the species in the community (Doser et al., 2023).

2.3 Single-species N-mixture models

The functions `NMix` and `spNMix` fit non-spatial and spatial N-mixture models in `spAbundance`. Following the N-mixture model structure of Royle (2004), we assume observers count the number of individuals of a target species at each site j over a set of multiple surveys $k = 1, \dots, K_j$, denoted as $y_k(\mathbf{s}_j)$. Note the number of surveys can vary by site, but at least some sites must be surveyed more than once to ensure identifiability. We model $y_k(\mathbf{s}_j)$ conditional on the true abundance of the species at site j , $N(\mathbf{s}_j)$, following

$$y_k(\mathbf{s}_j) \sim \text{Binomial}(N(\mathbf{s}_j), p_{j,k}), \quad (14)$$

where $p_{j,k}$ is the probability of detecting an individual given it is present at the site.

We model $p_{j,k}$ using a logit link function in which we can allow detection probability to vary over space and/or surveys. More specifically, we have

$$\text{logit}(p_{j,k}) = \mathbf{v}_{j,k}^\top \boldsymbol{\alpha}, \quad (15)$$

where $\boldsymbol{\alpha}$ is a vector of effects of covariates $\mathbf{v}(\mathbf{s}_j)$ (including an intercept). The model for abundance $N(\mathbf{s}_j)$ is identical to the single-species distance sampling model, which can include covariates and/or spatial random effects (Equations 1-3).

2.4 Multi-species N-mixture models

Analogous to HDS models, we can extend single-species N-mixture models to model abundance of a community of I total species (Yamaura et al., 2012). In multi-species N-mixture models, we estimate the abundance of species i at spatial location j , $N_i(\mathbf{s}_j)$. Our model for $N_i(\mathbf{s}_j)$ follows that of multi-species HDS models, such that expected abundance can be modeled as a function of species-specific effects of spatially-varying covariates (Equation 11) and species-specific random effects that can accommodate residual species correlations and residual spatial autocorrelation using a factor modeling approach (Equation 13). Species-specific covariate effects are modeled hierarchically following Equation 12. The observation portion of the multi-species N-mixture model is identical to the single-species model, now with species-specific covariate effects modeled hierarchically analogous to the abundance coefficients. `spAbundance` provides functions to fit non-spatial multi-species N-mixture models with (`lfMsNMix`) and without (`msNMix`) residual species correlations, as well as spatial multi-species N-mixture models that account for residual species correlations and spatial autocorrelation (`sfMsNMix`).

2.5 Single-species GLMMs

The functions `abund` and `spAbund` fit single-species (i.e., univariate) non-spatial and spatial GLMMs in `spAbundance` using abundance and related (e.g., biomass) data. As opposed to HDS and N-mixture models, GLMMs do not explicitly account for imperfect

detection via an additional hierarchical component to the model, and instead directly model the observed abundance at site j , $y(\mathbf{s}_j)$ to provide inference on relative abundance (e.g., Chapter 1 in [Kéry and Royle 2021](#)). Observed abundance $y(\mathbf{s}_j)$ is modeled using some probability distribution with mean $\mu(\mathbf{s}_j)$. **spAbundance** currently supports Poisson and negative binomial for use with count data and the Gaussian distribution for use with continuous abundance data (e.g., biomass). Mean relative abundance $\mu(\mathbf{s}_j)$ is modeled according to Equation 2 for the Poisson and negative binomial cases, while the log link function is removed for the Gaussian case. Note that variables thought to influence detection probability can be incorporated in the model for $\mu(\mathbf{s}_j)$ to improve estimates of relative abundance (e.g., random observer effects, [Link and Sauer 2002](#)).

2.6 Multi-species GLMMs

Now consider the case where we have count data for multiple species I at each survey location j , denoted $y_i(\mathbf{s}_j)$. We jointly model relative abundance of each species using a multivariate GLMM (e.g., [Warton et al. 2015](#); [Hui et al. 2015](#)), in which expected abundance for each species i at site j , $\mu_i(\mathbf{s}_j)$, is modeled analogous to Equations 11-13. Note the log link function is removed from Equation 11 when modeling abundance using a Gaussian distribution. As with HDS and N-mixture models, **spAbundance** provides functions to fit non-spatial multivariate GLMMs with (**lfMsAbund**) and without (**msAbund**) residual species correlations. Multivariate spatial GLMMs with residual species correlations are fit using the **sfMsAbund** function.

3 **spAbundance** functionality

Here we highlight the five main tasks performed by **spAbundance** (see Table 1 for function names).

1. *Data simulation.* The functions **simDS**, **simMsDS**, **simNMix**, **simMsNMix**, **simAbund**, and **simMsAbund** simulate data under the single-species and multi-species HDS, N-mixture, and GLMM frameworks for use in simulation studies or power analyses.

2. *Model fitting.* Model fitting functions were described previously (Section 2). All models are implemented in a Bayesian framework using custom Markov chain Monte Carlo (MCMC) algorithms written in C/C++ using R’s foreign language interface. **spAbundance** uses standard R formula syntax to specify abundance and detection probability models, with options to include random intercepts and random slopes using **lme4** syntax (Bates et al., 2015). Users can specify initial values for the MCMC algorithm as well as each parameter’s prior distribution to yield vague or informative priors as desired (Supplemental Information S1).

3. *Model validation and comparison.* The function **ppcAbund** performs posterior predictive checks on **spAbundance** model objects to assess model Goodness of Fit. The function **waicAbund** computes the conditional version (Millar, 2018) of the Widely Applicable Information Criterion (WAIC; Watanabe 2010) for model selection and assessment.

4. *Posterior summaries.* We include **summary** functions for **spAbundance** model objects that display concise summaries of the posterior distributions for estimated parameters as well as the potential scale reduction factor (\hat{R} ; Gelman and Rubin 1992) and effective sample size for convergence diagnostics. Simple **plot** functions allow for further convergence diagnostics via visual assessment of traceplots. The complete posterior samples are returned as **coda::mcmc** objects (Plummer et al., 2006)

5. *Prediction.* **predict** functions for all **spAbundance** model objects provide predictions of abundance across a user-specified set of locations (given covariate values and spatial coordinates). The resulting posterior predictive distributions can be used to generate abundance-based species distribution maps with associated uncertainty. Users can also predict detection probability for HDS and N-mixture models to yield insight on how detection probability varies across a user-specified range of covariate values.

4 Worked examples and online resources

We demonstrate **spAbundance** functionality with three worked examples and three vignettes. Complete details for all worked examples are provided in Supplemental Informa-

tion S1, along with associated code and data available on GitHub (https://github.com/doserjef/Doser_et_al_2023_spAbundance). The vignettes are provided in Supplemental Information S2-S4 as well as on the package website (<https://www.jeffdoser.com/files/spabundance-web/>). Here we provide a short overview of the worked examples and vignettes.

4.1 Case study 1: Bird density in central Florida

This case study demonstrates `spAbundance` functionality to fit spatial and nonspatial multi-species HDS models. We estimated density of 16 bird species in 2018 in the Disney Wilderness Preserve in central Florida, USA. Distance sampling data were collected as part of the National Ecological Observatory Network landbird monitoring program (Barnett et al., 2019). We compared the performance of the three multi-species model variants in `spAbundance` using WAIC. The spatial model substantially outperformed the non-spatial model with species correlations ($\Delta\text{WAIC} = 99$) and the non-spatial model without species correlations ($\Delta\text{WAIC} = 160$). Effects of forest cover on species-specific density varied across the community (Figure 1A), resulting in clear spatial variation in density of the 16 species (Supplemental Information S1 Figure S1). Detection probability quickly decayed with increasing distance from the observer (Figure 1B).

4.2 Case study 2: Black-throated Blue Warbler abundance in Hubbard Brook Experimental Forest

In this case study, we showcase how to fit spatial and nonspatial single-species N-mixture models. We estimated abundance of Black-throated Blue Warblers (*Setophaga caerulescens*) in the Hubbard Brook Experimental Forest in New Hampshire, USA using repeated count data from 2015 (Rodenhouse and Sillett 2021; Supplemental Information S1). We found minimal support for overdispersion and residual spatial autocorrelation, with a non-spatial Poisson N-mixture model performing best according to WAIC among multiple candidate models. A strong negative quadratic relationship with elevation revealed that abundance peaked at mid-elevations in the forest (Supplemental Information S1

Figure S2).

4.3 Case study 3: Forest biomass across the continental USA

Our final case study demonstrates how `spAbundance` can be used to fit models using “big data”. We estimated forest aboveground biomass across the continental US using data from $J = 86,933$ forest inventory plots (Figure 2A) collected via the US Forest Service Forest Inventory and Analysis Program (Bechtold and Patterson, 2005). We fit a spatially-explicit univariate GLMM using a Gaussian distribution with an ecoregion-specific random slope of tree canopy cover to reflect potential spatial variation in the relationship between canopy cover and biomass across different forest types. We found an overall positive relationship between tree canopy cover and biomass (median = 0.54 95% credible interval 0.43-0.66), but clear variation in the magnitude of the effect across ecoregions (Figure 2B). Biomass predictions across the US aligned with expectations, with highest biomass predicted in the Pacific Northwest (Figure 2C,D).

4.4 Vignettes

The three package vignettes provide complete details and examples for fitting all single-species and multi-species model types for HDS models (Supplemental Information S2), N-mixture models (Supplemental Information S3), and GLMMs (Supplemental Information S4). We provide extensive details on the required data formats for implementing the models in `spAbundance` and all function arguments including their default values. We additionally provide code to manipulate resulting objects after fitting models to generate a variety of plot types and summary figures.

5 Conclusions and future directions

The aim in developing `spAbundance` is to provide ecologists and conservation practitioners with a user-friendly tool to better quantify and understand spatial variation in the abundance of plant and animal populations. This R package fits Bayesian spatially-explicit

single-species and multispecies versions of three of the most common modeling frameworks for “unmarked” data types: hierarchical distance sampling models, N-mixture models, and generalized linear mixed models. By using efficient statistical algorithms implemented in C/C++ via R’s foreign language interface, **spAbundance** is capable of handling data sets with a large number of species (e.g., >100) and locations (e.g., 100,000). Our future aim is to add functionality for zero-inflated models and spatiotemporal models, including generalized HDS and N-mixture models (Chandler et al., 2011). Together, the package vignettes (Supplemental Information S2-S4), code to implement the three case studies (https://github.com/doserjef/Doser_et_al_2023_spAbundance), and the package website (<https://www.jeffdoser.com/files/spabundance-web/>) provide full details and thorough exposition of **spAbundance** model objects.

6 Data availability statement

The package **spAbundance** is available on the Comprehensive R Archive Network (CRAN; <https://cran.r-project.org/web/packages/spAbundance/index.html>). Data and code used in the examples are available on GitHub (https://github.com/doserjef/Doser_et_al_2023_spAbundance) and will be posted on Zenodo upon acceptance.

7 Acknowledgements

We thank J. Andrew Royle for helpful comments on the hierarchical distance sampling functionality and vignette. This work was supported by: E.F.Z. NSF grants DBI-1954406 and DEB-2213565; A.O.F. NASA CMS grants Hayes (CMS 2020) and Cook (CMS 2018), NSF grant DMS-1916395, joint venture agreements with the USDA Forest Service Forest Inventory and Analysis, USDA Forest Service Region 9 Forest Health Protection Northern Research Station.

8 Author Contributions

J.W.D. developed the package with insights from A.O.F; J.W.D. wrote the package vignettes with insights from M.K.; J.W.D. performed analyses and led writing of the manuscript with critical insights from E.F.Z., M.K., and A.O.F. All authors gave final approval for publication.

References

- Anderson, S. C., Ward, E. J., English, P. A., and Barnett, L. A. (2022). sdmTMB: an R package for fast, flexible, and user-friendly generalized linear mixed effects models with spatial and spatiotemporal random fields. *bioRxiv*.
- Banerjee, S., Carlin, B. P., and Gelfand, A. E. (2014). *Hierarchical modeling and analysis for spatial data*. Chapman and Hall/CRC.
- Banerjee, S. and Fuentes, M. (2012). Bayesian modeling for large spatial datasets. *WIREs Computational Statistics*, 4(1):59–66.
- Barker, R. J., Schofield, M. R., Link, W. A., and Sauer, J. R. (2018). On the reliability of N-mixture models for count data. *Biometrics*, 74(1):369–377.
- Barnett, D. T., Duffy, P. A., Schimel, D. S., Krauss, R. E., Irvine, K. M., Davis, F. W., Gross, J. E., Azuaje, E. I., Thorpe, A. S., Gudex-Cross, D., et al. (2019). The terrestrial organism and biogeochemistry spatial sampling design for the National Ecological Observatory Network. *Ecosphere*, 10(2):e02540.
- Bates, D., Mächler, M., Bolker, B., and Walker, S. (2015). Fitting linear mixed-effects models using lme4. *Journal of Statistical Software*, 67(1):1–48.
- Bechtold, W. A. and Patterson, P. L. (2005). *The enhanced forest inventory and analysis program—national sampling design and estimation procedures*. Number 80. USDA Forest Service, Southern Research Station.

- Buckland, S. T., Anderson, D. R., Burnham, K. P., Laake, J. L., Borchers, D. L., Thomas, L., et al. (2001). *Introduction to distance sampling: estimating abundance of biological populations*. Oxford (United Kingdom) Oxford Univ. Press.
- Carpenter, B., Gelman, A., Hoffman, M. D., Lee, D., Goodrich, B., Betancourt, M., Brubaker, M., Guo, J., Li, P., and Riddell, A. (2017). Stan: A probabilistic programming language. *Journal of Statistical Software*, 76(1).
- Chandler, R. B., Royle, J. A., and King, D. I. (2011). Inference about density and temporary emigration in unmarked populations. *Ecology*, 92(7):1429–1435.
- Datta, A., Banerjee, S., Finley, A. O., and Gelfand, A. E. (2016). Hierarchical nearest-neighbor Gaussian process models for large geostatistical datasets. *Journal of the American Statistical Association*, 111(514):800–812.
- de Valpine, P., Turek, D., Paciorek, C., Anderson-Bergman, C., Temple Lang, D., and Bodik, R. (2017). Programming with models: writing statistical algorithms for general model structures with NIMBLE. *Journal of Computational and Graphical Statistics*, 26:403–413.
- Doser, J. W., Finley, A. O., and Banerjee, S. (2023). Joint species distribution models with imperfect detection for high-dimensional spatial data. *Ecology*, 104(9):e4137.
- Doser, J. W., Finley, A. O., Kéry, M., and Zipkin, E. F. (2022). spOccupancy: An R package for single-species, multi-species, and integrated spatial occupancy models. *Methods in Ecology and Evolution*, 13(8):1670–1678.
- Finley, A. O., Banerjee, S., and Gelfand, A. E. (2015). spBayes for Large Univariate and Multivariate Point-Referenced Spatio-Temporal Data Models. *Journal of Statistical Software*, 63(13):1–28.
- Finley, A. O., Datta, A., Cook, B. D., Douglas C. Morton, H. E. A., and Banerjee, S. (2019). Efficient algorithms for Bayesian Nearest Neighbor Gaussian Processes. *Journal of Computational and Graphical Statistics*, 28(2):401–414.

- Fiske, I. and Chandler, R. (2011). unmarked: an R package for fitting hierarchical models of wildlife occurrence and abundance. *Journal of Statistical Software*, 43(10):1–23.
- Gelman, A. and Rubin, D. B. (1992). Inference from iterative simulation using multiple sequences. *Statistical Science*, 7(4):457–472.
- Goldstein, B. R. and de Valpine, P. (2022). Comparing N-mixture models and GLMMs for relative abundance estimation in a citizen science dataset. *Scientific Reports*, 12(1):12276.
- Guélat, J. and Kéry, M. (2018). Effects of spatial autocorrelation and imperfect detection on species distribution models. *Methods in Ecology and Evolution*, 9(6):1614–1625.
- Hodges, J. S. and Reich, B. J. (2010). Adding spatially-correlated errors can mess up the fixed effect you love. *The American Statistician*, 64(4):325–334.
- Hogan, J. W. and Tchernis, R. (2004). Bayesian factor analysis for spatially correlated data, with application to summarizing area-level material deprivation from census data. *Journal of the American Statistical Association*, 99(466):314–324.
- Hui, F. K., Taskinen, S., Pledger, S., Foster, S. D., and Warton, D. I. (2015). Model-based approaches to unconstrained ordination. *Methods in Ecology and Evolution*, 6(4):399–411.
- Kellner, K. F., Fowler, N. L., Petroelje, T. R., Kautz, T. M., Beyer Jr, D. E., and Belant, J. L. (2021). ubms: An R package for fitting hierarchical occupancy and N-mixture abundance models in a Bayesian framework. *Methods in Ecology and Evolution*, 13(3):577–584.
- Kéry, M. and Royle, J. A. (2021). *Applied hierarchical modeling in ecology: Analysis of distribution, abundance, and species richness in R and BUGS: Volume 2: Dynamic and advanced models*. Academic Press.
- Link, W. A. and Sauer, J. R. (2002). A hierarchical analysis of population change with application to cerulean warblers. *Ecology*, 83(10):2832–2840.

- Lopes, H. F. and West, M. (2004). Bayesian model assessment in factor analysis. *Statistica Sinica*, pages 41–67.
- Millar, R. B. (2018). Conditional vs marginal estimation of the predictive loss of hierarchical models using WAIC and cross-validation. *Statistics and Computing*, 28(2):375–385.
- Miller, D. L., Burt, M. L., Rexstad, E. A., and Thomas, L. (2013). Spatial models for distance sampling data: recent developments and future directions. *Methods in Ecology and Evolution*, 4(11):1001–1010.
- Nichols, J. D., Thomas, L., and Conn, P. B. (2009). Inferences about landbird abundance from count data: recent advances and future directions. *Modeling demographic processes in marked populations*, pages 201–235.
- Plummer, M., Best, N., Cowles, K., and Vines, K. (2006). CODA: Convergence Diagnosis and Output Analysis for MCMC. *R News*, 6(1):7–11.
- Rodenhouse, N. L. and Sillett, T. S. (2021). Valley-wide Bird Survey, Hubbard Brook Experimental Forest, 1999-2016 (ongoing). <https://doi.org/10.6073/pasta/faca2b2cf2db9d415c39b695cc7fc21>. Accessed: 2021-09-07.
- Royle, J. A. (2004). N-mixture models for estimating population size from spatially replicated counts. *Biometrics*, 60(1):108–115.
- Royle, J. A., Dawson, D. K., and Bates, S. (2004). Modeling abundance effects in distance sampling. *Ecology*, 85(6):1591–1597.
- Sollmann, R., Gardner, B., Williams, K. A., Gilbert, A. T., and Veit, R. R. (2016). A hierarchical distance sampling model to estimate abundance and covariate associations of species and communities. *Methods in Ecology and Evolution*, 7(5):529–537.
- Taylor-Rodriguez, D., Finley, A. O., Datta, A., Babcock, C., Andersen, H.-E., Cook, B. D., Morton, D. C., and Banerjee, S. (2019). Spatial factor models for high-

- dimensional and large spatial data: An application in forest variable mapping. *Statistica Sinica*, 29:1155.
- Tikhonov, G., Opedal, Ø. H., Abrego, N., Lehtikoinen, A., de Jonge, M. M., Oksanen, J., and Ovaskainen, O. (2020). Joint species distribution modelling with the r-package Hmsc. *Methods in Ecology and Evolution*, 11(3):442–447.
- Tobler, M. W., Kéry, M., Hui, F. K., Guillerá-Arroita, G., Knaus, P., and Sattler, T. (2019). Joint species distribution models with species correlations and imperfect detection. *Ecology*, 100(8):e02754.
- Ver Hoef, J. M., Peterson, E. E., Hooten, M. B., Hanks, E. M., and Fortin, M.-J. (2018). Spatial autoregressive models for statistical inference from ecological data. *Ecological Monographs*, 88(1):36–59.
- Vieilledent, G. (2019). *hSDM: Hierarchical Bayesian Species Distribution Models*. R package version 1.4.1.
- Warton, D. I., Blanchet, F. G., O’Hara, R. B., Ovaskainen, O., Taskinen, S., Walker, S. C., and Hui, F. K. (2015). So many variables: Joint modeling in community ecology. *Trends in Ecology & Evolution*, 30(12):766–779.
- Watanabe, S. (2010). Asymptotic equivalence of Bayes cross validation and widely applicable information criterion in singular learning theory. *Journal of Machine Learning Research*, 11(12).
- Yamaura, Y., Royle, J. A., Shimada, N., Asanuma, S., Sato, T., Taki, H., and Makino, S. (2012). Biodiversity of man-made open habitats in an underused country: a class of multispecies abundance models for count data. *Biodiversity and Conservation*, 21:1365–1380.

Tables and Figures

Table 1: List of core functions in the **spAbundance** package.

Functionality	Description
Data simulation	
<code>simDS</code>	Simulate single-species distance sampling data
<code>simMsDS</code>	Simulate multi-species distance sampling data
<code>simNMix</code>	Simulate single-species repeated count data with imperfect detection
<code>simMsNMix</code>	Simulate multi-species repeated count data with imperfect detection
<code>simAbund</code>	Simulate single-species count data with perfect detection.
<code>simMsAbund</code>	Simulate multi-species count data with perfect detection.
Model fitting	
<code>DS</code>	Single-species HDS model
<code>spDS</code>	Single-species spatial HDS model
<code>msDS</code>	Multi-species HDS model
<code>lfMsDS</code>	Multi-species HDS model with species correlations
<code>sfMsDS</code>	Multi-species spatial HDS model with species correlations
<code>NMix</code>	Single-species N-mixture model
<code>spNMix</code>	Single-species spatial N-mixture model
<code>msNMix</code>	Multi-species N-mixture model
<code>lfMsNMix</code>	Multi-species N-mixture model with species correlations
<code>sfMsNMix</code>	Spatial multi-species N-mixture model with species correlations
<code>abund</code>	Single-species GLMM
<code>spAbund</code>	Single-species spatial GLMM
<code>msAbund</code>	Multi-species GLMM
<code>lfMsAbund</code>	Multi-species GLMM with species correlations
<code>sfMsAbund</code>	Multi-species spatial GLMM with species correlations
Model assessment	
<code>ppcAbund</code>	Posterior predictive check using Bayesian p-values
<code>waicAbund</code>	Compute Widely Applicable Information Criterion

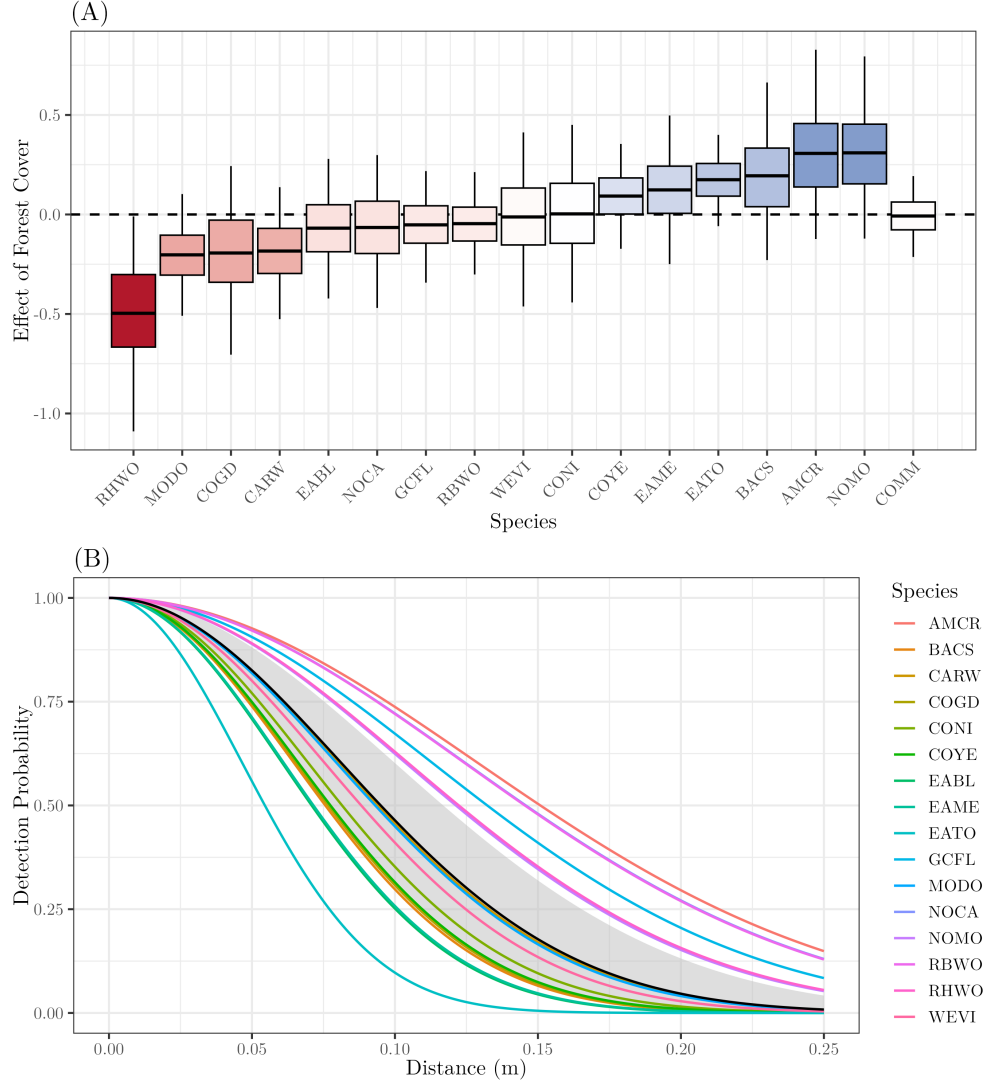


Figure 1: Species-specific effects of forest cover on density (A) and relationship between detection probability and distance from the observer (B) in the central Florida bird case study. Panel (A) shows the estimated mean (dark line), 50% credible interval (box), and 95% credible interval (whiskers) for the effect of forest cover on the overall community (COMM) and 16 individual species. In Panel (B), lines represent posterior mean detection probabilities for each species. The black line represents the average across the community (i.e., the community-level effect), and the grey region is the associated 95% credible interval. See Supplemental Information S1 for species code definitions.

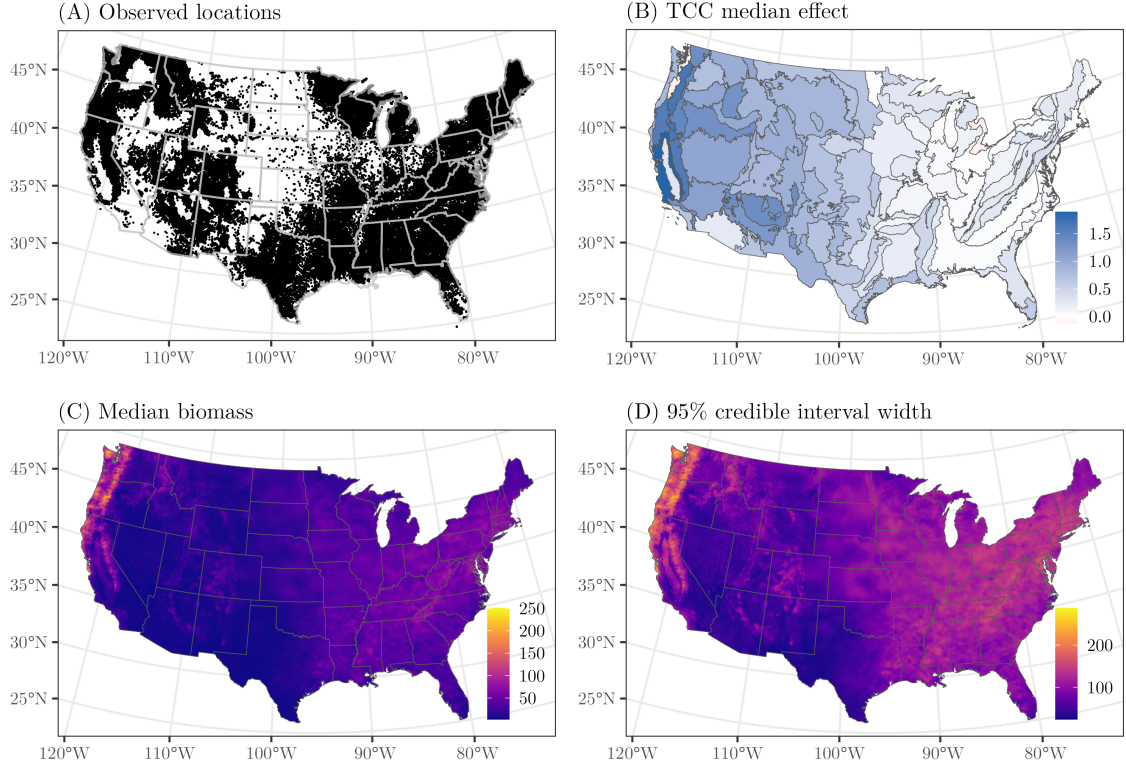


Figure 2: Data and predictions from the forest biomass case study. Panel A shows the observed locations of the 86,933 Forest Inventory and Analysis plots. Note these are the publicly available perturbed locations in which FIA adds a small amount of random noise to the true plot locations. Panel B shows the estimated random effect of tree canopy cover on forest biomass within distinct ecoregions. Panel C shows predicted biomass (posterior median) across the continental USA (tons per acre), with associated uncertainty (95% credible interval width) in Panel D.

Supplemental Information S1 for spAbundance: An R package for single-species and multi-species spatially-explicit abundance models

Table S1: Comparison of functionality to fit hierarchical distance sampling (HDS) models, N-mixture models, and generalized linear mixed models (GLMMs) in multiple R packages commonly used in ecology. NB indicates functionality to model abundance with a negative binomial distribution. Note that this is not an exhaustive comparison of package functionality, but rather a comparison of functionality for fitting spatially-explicit single-species and multi-species abundance models using count data.

Package	HDS	N-mixture	GLMM	Spatial	Multi-species	NB	LMM
spAbundance	✓	✓	✓	✓	✓	✓	✓
hSDM		✓	✓	✓			
ubms	✓	✓		✓			
unmarked	✓	✓				✓	
sdmTMB			✓	✓		✓	✓
spBayes			✓	✓	✓		✓
HMSC			✓	✓	✓	✓	✓
dsm	✓			✓		✓	

1 Additional statistical details

1.1 Nearest Neighbor Gaussian Process

Let $\mathcal{L} = \{\mathbf{s}_1, \mathbf{s}_2, \dots, \mathbf{s}_J\}$ be the set of sampled spatial locations, and define \mathbf{w} as a $J \times 1$ vector of spatial random effects. We envision $w(\mathbf{s}_j)$ as a realization of a smooth latent surface $\{w(\mathbf{s}) \mid \mathbf{s} \in \mathcal{D}\}$, where \mathcal{D} is the geographical domain of interest. First, suppose Gaussian Processes (GPs) are used to model \mathbf{w} , as is common throughout the spatial statistics literature (e.g., [Banerjee et al. 2014](#)). By definition, a GP model for $\{w(\mathbf{s})\}$ implies that for any finite set of locations \mathcal{L} , the vector of random effects \mathbf{w} follows a zero-mean multivariate Gaussian distribution with a $J \times J$ covariance matrix $\mathbf{C}(\mathbf{s}, \mathbf{s}', \boldsymbol{\theta})$ that is a function of the distances between any pair of site coordinates \mathbf{s} and \mathbf{s}' and a set of parameters ($\boldsymbol{\theta}$) that govern the spatial process according to a parametric covariance

function. $\boldsymbol{\theta}$ consists of a spatial variance (σ^2) and spatial decay (ϕ) parameter for the exponential, spherical, and Gaussian covariance functions, and additionally includes a spatial smoothness parameter ν for the Matérn covariance function.

Both frequentist and Bayesian estimation of spatial models using GPs requires taking the inverse and determinant of a dense $J \times J$ covariance matrix (i.e., $\mathbf{C}(\mathbf{s}, \mathbf{s}', \boldsymbol{\theta})$) that involves $O(J^3)$ computations (floating point operations or FLOPs), which quickly renders such an approach impractical for even moderately sized data sets (i.e., hundreds of spatial locations). In **spAbundance**, we replace the GP prior for the spatial random effects with a Nearest Neighbor Gaussian Process (NNGP) prior (Datta et al., 2016). The NNGP is a valid GP that is based on writing the full multivariate Gaussian distribution for \mathbf{w} as a product of conditional densities, such that

$$p(\mathbf{w}) = p(\mathbf{w}(\mathbf{s}_1)) \cdot p(\mathbf{w}(\mathbf{s}_2) \mid \mathbf{w}(\mathbf{s}_1)) \cdots p(\mathbf{w}(\mathbf{s}_J) \mid \mathbf{w}(\mathbf{s}_{J-1}), \dots, \mathbf{w}(\mathbf{s}_1)), \quad (\text{S1})$$

where $p(\cdot)$ denotes a probability density function. The NNGP prior achieves computational efficiency by replacing the conditioning sets on the right-hand side of (S1) with a set of new conditioning sets, whose maximum size is determined by a pre-specified number of neighbors, m , where $m \ll J$. Datta et al. (2016) showed that $m = 15$ provides nearly identical inference to the full GP under a variety of scenarios. Let $n(\mathbf{s}_j)$ denote the set of at most m neighbors for location \mathbf{s}_j . Following Vecchia (1988), we set $n(\mathbf{s}_j)$ to be the set of at most m nearest neighbors of \mathbf{s}_j from $\{\mathbf{s}_1, \mathbf{s}_2, \dots, \mathbf{s}_{j-1}\}$ with respect to Euclidean distance. Note, this requires the set of \mathcal{L} locations to have some prespecified ordering. In **spAbundance**, we order the coordinates along the horizontal axis.

Through careful construction of the neighbor sets and set of spatial locations as a directed acyclic graph, Gaussian distribution theory reveals the NNGP prior yields a new joint density for \mathbf{w} , denoted $\tilde{p}(\mathbf{w})$. Let $\mathbf{w}(n(\mathbf{s}_j))$ denote the at most m realizations of the NNGP at the locations in the neighbor set $n(\mathbf{s}_j)$. Let $C(\cdot, \boldsymbol{\theta})$ denote the covariance function of the original Gaussian Process (GP) from which the NNGP is derived. For any two sets A_1 and A_2 , define $C_{A_1, A_2}(\boldsymbol{\theta})$ as the covariance matrix between the observations

in A_1 and A_2 . Our NNGP prior for \mathbf{w} thus takes the form

$$\tilde{p}(\mathbf{w}) = \prod_{j=1}^J \text{Normal}(\mathbf{w}(\mathbf{s}_j) \mid \mathbf{w}(n(\mathbf{s}_j))\mathbf{b}(\mathbf{s}_j), \mathbf{f}(\mathbf{s}_j)), \quad (\text{S2})$$

where $\mathbf{b}(\mathbf{s}_j)$ is defined as

$$\mathbf{b}(\mathbf{s}_j) = \mathbf{C}_{\mathbf{s}_j, n(\mathbf{s}_j)}(\boldsymbol{\theta}) \mathbf{C}_{n(\mathbf{s}_j), n(\mathbf{s}_j)}^{-1}(\boldsymbol{\theta}), \quad (\text{S3})$$

with $\mathbf{b}(\mathbf{s}_1) = \mathbf{0}$, and $\mathbf{f}(\mathbf{s}_j)$ is defined as

$$\mathbf{f}(\mathbf{s}_j) = \mathbf{C}_{\mathbf{s}_j, \mathbf{s}_j}(\boldsymbol{\theta}) - \mathbf{C}_{\mathbf{s}_j, n(\mathbf{s}_j)}(\boldsymbol{\theta}) \mathbf{C}_{n(\mathbf{s}_j), n(\mathbf{s}_j)}^{-1}(\boldsymbol{\theta}) \mathbf{C}_{n(\mathbf{s}_j), \mathbf{s}_j}(\boldsymbol{\theta}). \quad (\text{S4})$$

1.2 Detection functions in hierarchical distance sampling models

spAbundance currently supports two detection functions for single-species and multi-species hierarchical distance sampling models: the half-normal and negative exponential. Both functions are controlled by a scale parameter, σ_j , which controls the rate of distance-dependent decay in detection probability. For distance x , the half-normal detection function takes the form

$$g(x) = \exp\left(-\frac{x^2}{2\sigma_j^2}\right). \quad (\text{S5})$$

The negative exponential detection function takes the form

$$g(x) = \exp\left(-\frac{x}{\sigma_j}\right). \quad (\text{S6})$$

1.3 Prior distributions in **spAbundance**

The prior distributions in **spAbundance** are sufficiently flexible to allow for vague or weakly informative priors, as well as informative priors if such information is available. **spAbundance** by default will assign default values for all hyperparameters in the prior

distributions, which result in weakly informative priors. The `priors` argument in all model fitting functions allows users to explicitly specify the hyperparameter values for all prior distributions. When prior distributions are not explicitly specified by the user, the default values used for the hyperparameter values in the priors will be reported to the screen. Below we describe the prior distribution for each individual parameter, as well as our choice for the default hyperparameter values for the priors in `spAbundance`.

1.4 Single-species models

We assign Gaussian (i.e., normal) priors to the abundance (β) and detection (α) regression coefficients (for HDS and N-mixture models). Gaussian priors are a common choice for prior distributions on regression coefficients (Gelman et al., 2014). Our default prior on the abundance regression coefficients (β) is a normal distribution with a mean of 0 and variance of 100, which results in a vague prior distribution that has a small impact on the resulting posterior estimate. The same prior is also used for detection regression coefficients (α) in hierarchical distance sampling models. For the detection regression coefficients in N-mixture models, `spAbundance` will by default set the mean to 0 and variance to 2.72. This results in a relatively flat prior across the probability scale (e.g., (Northrup and Gerber, 2018)).

For the spatial parameters in all spatially-explicit models, priors must be at least weakly informative for the model to identify the spatial decay (ϕ) and spatial variance parameters (σ^2 ; Banerjee et al. 2014). Accordingly, we follow standard recommendations from the spatial statistics literature for placing priors on the spatial variance (σ^2), spatial decay (ϕ), and spatial smoothness (ν) parameter, where the spatial smoothness parameter only applies if using a Matérn covariance function (Banerjee et al., 2014). Specifically, we place an inverse-Gamma prior on the spatial variance and uniform priors on the spatial decay (and smoothness parameter if applicable). For the spatial variance parameter, we suggest following recommendations from Banerjee et al. 2014 and setting the shape parameter to 2 and the scale parameter equal to our best guess of the spatial variance. By default, `spAbundance` will set the shape parameter to 2 and the scale parameter to 1.

This weakly informative prior suggests a prior mean of 1 for the spatial variance. For the spatial decay parameter, we assume a uniform prior, again following [Banerjee et al. 2014](#). By default, we set the lower and upper bounds of the spatial decay parameter based on the minimum and maximum distances between sites in the data. More specifically, the default prior values set the lower bound to $3/\max$ and the upper bound to $3/\min$, where \min and \max are the minimum and maximum distances between sites in the data set, respectively. This equates to a vague prior that states that spatial autocorrelation in the spatial random effects could only be between sites that are very close to each other, or could span across the entire observed study area. If additional information is known on the extent of spatial autocorrelation in the data, the user may place more restrictive bounds on the uniform prior, which would reduce the amount of time needed for adequate mixing and convergence of the MCMC chains. We do not set default bounds on the spatial smoothness parameter, ν , and rather require the user to specify these bounds if a Matérn correlation function is used.

We assign a uniform distribution for the negative binomial dispersion parameter κ when fitting models in **spAbundance** with a negative binomial distribution. By default, we set the lower bound of the uniform distribution to 0 and the upper bound of the uniform distribution to 100. Recall that smaller values of κ indicate overdispersion in the abundance values relative to a Poisson model, while higher values indicate minimal overdispersion in abundance. In particular, as $\kappa \rightarrow \infty$, the negative binomial distribution becomes the Poisson distribution. When there is little support for overdispersion in abundance relative to the Poisson distribution, the estimates of κ will likely approach the upper bound of the uniform prior distribution. When the upper bound of the uniform distribution is substantially high (e.g., the default value of 100), this is a good indication that there is little support for overdispersion, and that model selection criteria (e.g., WAIC) will likely favor the simpler Poisson distribution.

When fitting GLMMs with a Gaussian distribution, we assign an inverse-Gamma prior to the residual variance parameter τ^2 . Our default hyperparameter values are 0.01 and 0.01 for both the shape and scale parameters, which corresponds to a vague prior such

that the estimated value is almost entirely informed by the data alone.

When fitting models with random intercepts and/or slopes in `spAbundance`, we use inverse-Gamma priors for any random effect variances on abundance (σ_μ^2) and/or detection (σ_p^2). Following the recommendations of [Lunn et al. \(2013\)](#), by default we set the scale and shape hyperparameters to 0.1, which results in a weakly informative prior on the random effect variances. This prior can result in shrinkage of the random effect values towards zero under certain circumstances ([Gelman, 2006](#)), although this primarily only occurs when the number of levels in the random effect is small (e.g., less than 10). Future versions of the package will also allow for half-Cauchy priors on the random effect variance parameters, which has been shown to perform better than the inverse-Gamma prior in situations where the random effect has very few levels ([Gelman, 2006](#)).

1.5 Multi-species models

We assign Gaussian priors to the community-level occurrence (μ_β) and detection (μ_α) mean regression parameters. Following the same logic as presented in Section 1.4 for single-species models, we set the prior mean to 0 and the prior variance to 100 for the abundance parameters, and the prior variance to 2.72 for the detection parameters.

For the community-level abundance (τ_β^2) and detection (τ_α^2) variance parameters, we assign inverse-Gamma priors. As described for the random effect variances in the single-species models in Section 1.4, we by default set the scale and shape parameters to 0.1.

Uniform priors are specified for the species-specific negative binomial dispersion parameters using the same default hyperparameter values as the single-species case. Inverse-gamma priors are again used for the species-specific Gaussian residual variance parameters, with default shape and scale hyperparameters set to 0.01. Inverse-Gamma priors are again used for random effect variances for any additional random effects included in the multi-species models. Hyperparameter values are by default set to 0.1.

For models accounting for residual species autocorrelation using a factor modeling approach, we require additional constraints to ensure identifiability of the species-specific factor loadings from the latent factors ([Papastamoulis and Ntzoufras, 2022](#)). Following

[Aguilar and West \(2000\)](#) and [Taylor-Rodriguez et al. \(2019\)](#), we set all elements in the upper triangle of the $I \times q$ factor loadings matrix $\mathbf{\Lambda}$ equal to 0 and its diagonal elements equal to 1. We assign standard normal prior distributions (i.e., a normal prior distribution with mean 0 and variance 1) to all elements in $\mathbf{\Lambda}$ below the upper diagonal. For spatially-explicit multi-species models, we assign a uniform prior to each of the q spatial decay parameters in ϕ . We use the same default hyperparameter values as those described for the single-species models.

2 Case Study 1: Bird density in south-central Florida

In our first case study, we estimated density of 16 bird species in 2018 in the Disney Wilderness Preserve in central Florida, USA using a spatial multi-species distance sampling model. These data were collected as part of the National Ecological Observatory Network landbird monitoring program ([Barnett et al., 2019](#)). Observers recorded the number of all bird species detected during a six-minute, unlimited radius point count survey at 90 sites. The distance of each individual bird to the observer was recorded using a laser rangefinder. We only used observations within 250m and subsequently binned the distance measurements into four distance bands (0-25m, 25-50m, 50-100m, 100-250m). We removed all species with less than 10 observations, resulting in a total of 16 species. We modeled abundance as a function of forest cover and grassland cover, and modeled detection probability as a function of wind. Forest cover and grassland cover were calculated from the USGS EROS (Earth Resources Observation and Science) Center, which produces high-resolution (250m) annual land cover maps across the continental US that are backcasted to 1938 ([Sohl et al., 2016](#)). We calculated the proportion of grassland and forest cover within 1km of each point count survey location. All covariates were standardized to have a mean of 0 and standard deviation of 1. We compared the performance of three multi-species distance sampling models: (1) a non-spatial model without species correlations using `msDS`; (2) a non-spatial model with species correlations using `lfmsDS`; and (3) a spatial model with species correlations using `sfmsDS`. We used

two latent factors for the models that included species correlations, as exploratory data analysis revealed models with more factors did not converge due to the large number of rare species in the data set. We used a NNGP with 15 neighbors for the spatially-explicit model (as recommended in [Datta et al. 2016](#)). We ran all models for three chains of 100,000 iterations with a burn-in period of 50,000 iterations and a thinning rate of 50, resulting in a total of 3000 samples from the posterior distribution. Convergence was assessed using visual assessment of trace plots, the potential scale reduction factor (\hat{R}), and effective sample size. Model run times to run three chains in sequence each with 100,000 MCMC samples were 29 minutes for the non-spatial model, 39 minutes for the non-spatial model with species-correlations, and 56 minutes for the spatial model. Models were fit using a single CPU on a computer running a Linux operating system with an Intel 3.8 GHz i7-7700HQ 4-core processor and 16GB RAM.

The spatial multi-species HDS model substantially outperformed both the non-spatial HDS model with species correlations ($\Delta\text{WAIC} = 99$) and the non-spatial HDS model without species correlations ($\Delta\text{WAIC} = 160$). Maps of density predicted across the preserve show substantial spatial variation in density both within and across species (Figure S1). We found small yet variable effects of forest cover on density across the 16 species, which resulted in a community-level average effect at essentially 0 (Figure 1A main text). Detection probability quickly decayed with increasing distance from the observer (Figure 1B main text).

Species codes shown in Figure 1 in the main manuscript are: AMCR (American Crow), BACS (Bachman’s Sparrow), CARW (Carolina Wren), COGD (Common Ground-Dove), CONI (Common Nighthawk), COYE (Common Yellowthroat), EABL (Eastern Bluebird), EAME (Eastern Meadowlark), EATO (Eastern Towhee), GCFL (Great-crested Flycatcher), MODO (Mourning Dove), NOCA (Northern Cardinal), NOMO (Northern Mockingbird), RBWO (Red-bellied Woodpecker), RHWO (Red-headed Woodpecker), WEVI (White-eyed Vireo).

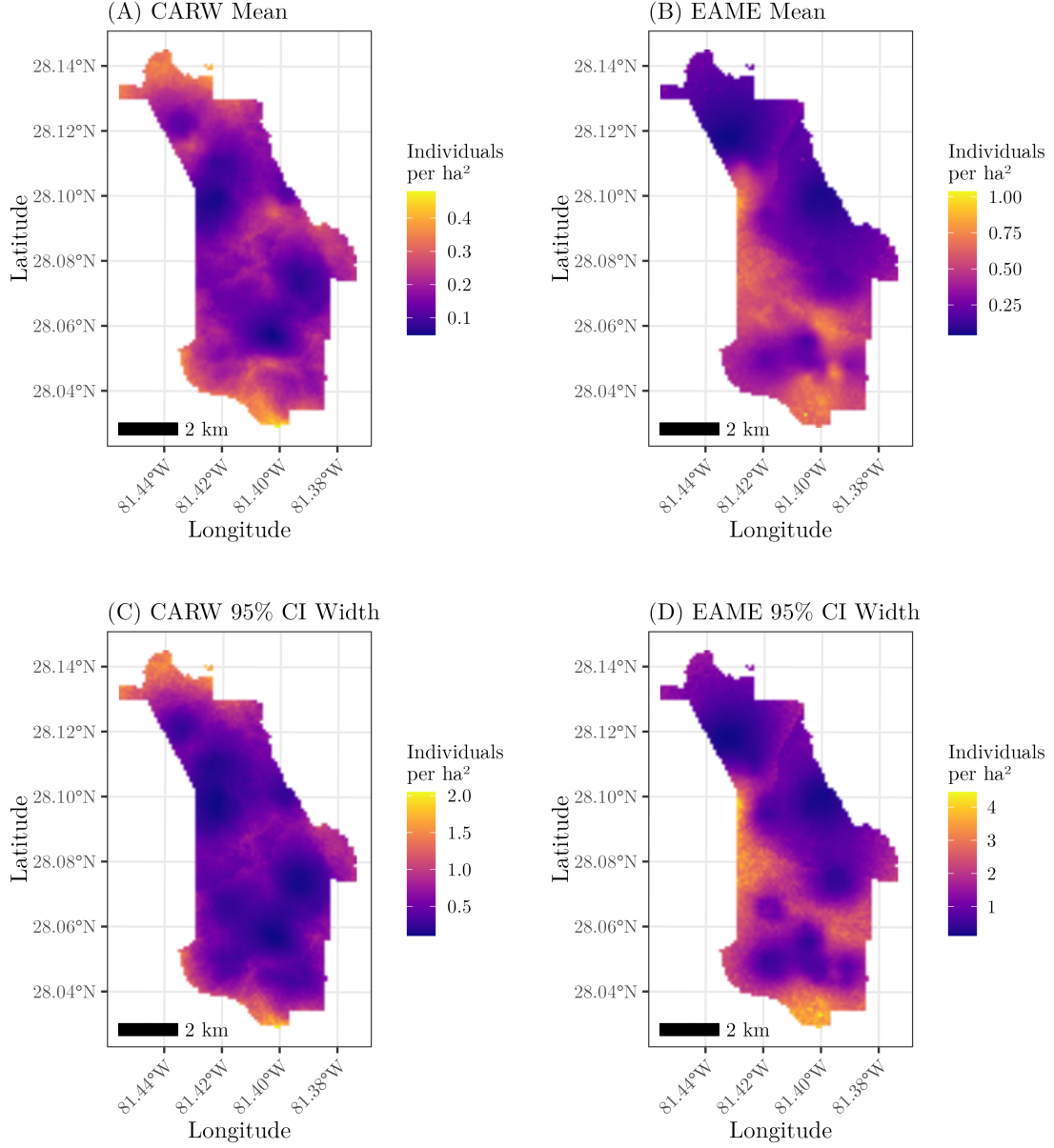


Figure S1: Density estimates (posterior means) and corresponding uncertainty (95% credible interval widths) for (A, C) Carolina Wren (*Thryothorus ludovicianus*; CARW) and (B, D) Eastern Meadowlark (*Sturnella magna*; EAME) across the Disney Wilderness Preserve using a spatial multi-species distance sampling model that accounts for residual species correlations.

3 Case Study 2: Black-throated Blue Warbler abundance in Hubbard Brook Experimental Forest

In this case study, we estimated abundance of Black-throated Blue Warblers (*Setophaga caerulescens*) in the Hubbard Brook Experimental Forest in New Hampshire, USA (Rodenhouse and Sillett, 2021) using nonspatial and spatial N-mixture models. Data were collected using standard point count surveys at 373 sites three times during the breeding season in 2015. Some sites were not sampled for all three surveys, resulting in an imbalanced data set. During each survey observers recorded the number of individuals of all bird species within a 50m radius circle. We included time of day (linear) and day of year (linear and quadratic) as fixed effects in the detection portion of the model, and specified linear and quadratic effects of elevation as abundance predictors. We compared the performance of four models: (1) a non-spatial Poisson N-mixture model; (2) a non-spatial negative binomial N-mixture model; (3) a spatial Poisson N-mixture model; and (4) a spatial negative binomial N-mixture model. Model performance was compared using WAIC. We ran all four candidate models for three chains of 125,000 MCMC samples discarding 85,000 samples as burn-in and using a thinning rate of 20 for a total of 6000 posterior samples. After model fitting, we subsequently predicted abundance across the Hubbard Brook Experimental Forest using the top performing model to generate a map of Black-throated Blue Warbler abundance across the forest. Model run times to complete all three chains run in sequence using a single CPU were 7.9 minutes for the non-spatial Poisson model, 10.6 minutes for the non-spatial negative binomial model, 18.8 minutes for the spatial Poisson model, and 20.3 minutes for the spatial negative binomial model. Models were fit on a computer running a Linux operating system with an Intel 3.8 GHz i7-7700HQ 4-core processor and 16GB RAM.

We found little support for overdispersion or residual spatial autocorrelation in model estimates of Black-throated Blue Warbler abundance. The non-spatial and spatial Poisson N-mixture models had nearly identical WAIC values (WAIC = 2204), while the Poisson N-mixture models slightly outperformed both the non-spatial (WAIC = 2207) and spatial

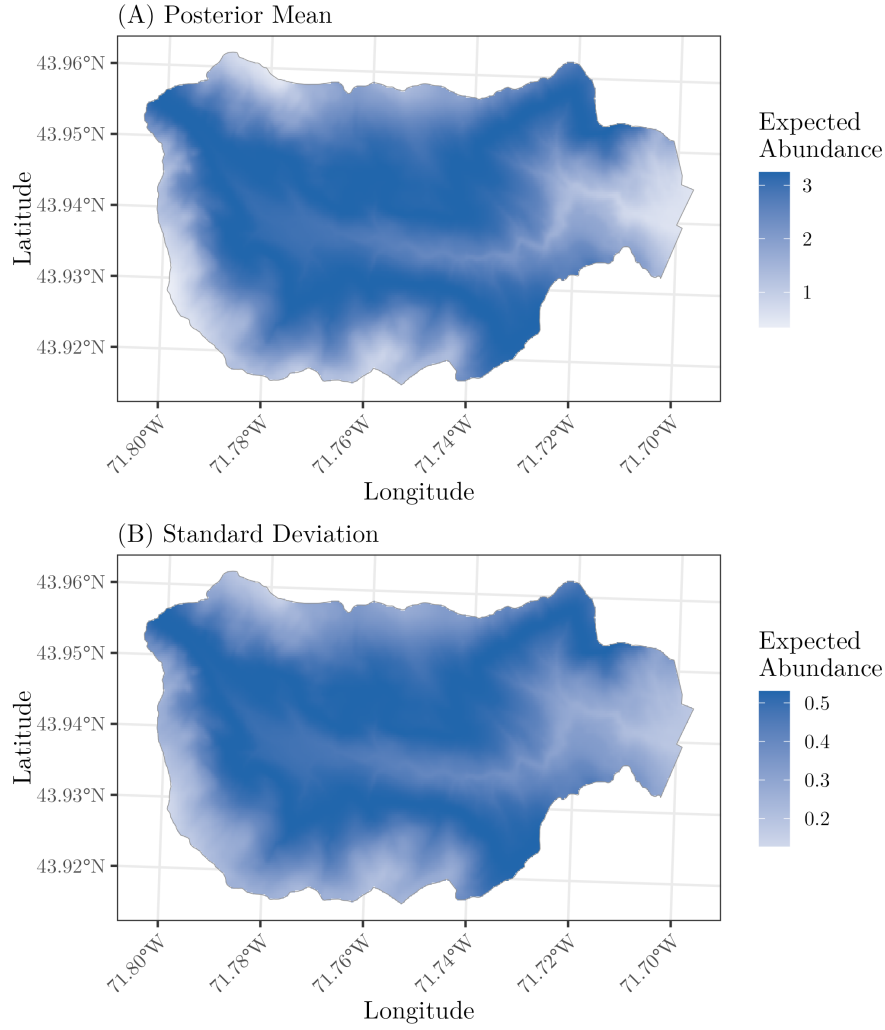


Figure S2: Estimated abundance of Black-throated Blue Warblers (*Setophaga caerulescens*) in 2015 across the Hubbard Brook Experimental Forest in New Hampshire, USA. Panel (A) shows posterior means and panel (B) shows posterior standard deviation. Estimates come from the top-performing model according to WAIC (a non-spatial Poisson N-mixture model).

(WAIC = 2208) negative binomial N-mixture models. We present model results for the non-spatial Poisson N-mixture model. Abundance had a strong negative quadratic relationship with elevation (Table S2), indicating Black-throated Blue Warbler abundance peaks at mid-elevations in the region. Detection probability showed a positive, linear relationship with the day of year, indicating higher detection probability of individuals later in the breeding season. Predictions of abundance across Hubbard Brook showcase the strong relationship between abundance and elevation (Figure S2).

Table S2: Parameter estimates from a non-spatial Poisson N-mixture model for estimating Black-throated Blue Warbler abundance in 2015 across Hubbard Brook Experimental Forest in New Hampshire, USA.

	Mean	SD	2.5% Quantile	97.5% Quantile
Abundance				
Intercept	1.16	0.16	0.88	1.50
Elevation (linear)	-0.06	0.055	-0.17	0.04
Elevation (quadratic)	-0.30	0.05	-0.40	-0.21
Detection				
Intercept	-0.89	0.21	-1.34	-0.50
Day (linear)	0.16	0.05	0.07	0.25
Day (quadratic)	-0.08	0.055	-0.18	0.03
Time of day	-0.02	0.05	-0.11	0.07

4 Case study 3: Forest biomass across the continental USA

In our final case study, we showcase `spAbundance` functionality for fitting spatial linear mixed models with a “big” spatial data set. Specifically, we estimated forest aboveground biomass (AGB) across the continental US with data from $J = 86,933$ forest inventory plots. Biomass is a sensible measure of abundance that is widely used for modeling plant distributions, especially in forestry applications across large spatial scales. These data come from the Forest Inventory and Analysis monitoring program of the US Forest Service (Bechtold and Patterson, 2005). Permanent field plot locations were established based on an equal probability sampling design (Bechtold and Patterson, 2005), with each field plot visited on a five-year cycle for the eastern US and a ten-year cycle for the western US. Field crews record stem measurements for all trees with diameter at breast height of 12.7cm or greater, and well-established allometric equations were used to estimate forest biomass for each plot. Here we extracted plot-level biomass (tons per acre) from the most recent cycle across the continental US. For this illustrative analysis, we used the publicly available perturbed plot coordinates (i.e., FIA adds a small amount of random noise to plot locations to protect ownership privacy and ensure ecological integrity). AGB takes positive, continuous values, and so we square root transformed

biomass values for use as our response variable to ensure positive support of biomass values after back transformation and to meet basic linear model assumptions. We modeled square-root transformed biomass using a GLMM with a Gaussian distribution (i.e., a linear mixed model). Mean square-root transformed biomass was modeled as a function of three covariates: elevation (linear), 30-year maximum temperature climate normal (linear and quadratic), and tree canopy cover in 2021 (linear). Elevation data were accessed from Terrain Tiles on August 17, 2022 from <https://registry.opendata.aws/terrain-tiles>. We obtained climate normals from TerraClimate (Abatzoglou et al., 2018) and tree canopy cover from NLCD (Coulston et al., 2012; Dewitz, 2023). We compared four candidate models: (1) a linear mixed model with a random intercept of ecoregion as a simple approach to accommodate spatial variation in biomass across environmentally distinct regions; (2) a linear mixed model with an ecoregion random intercept and an ecoregion-specific random slope of tree canopy cover to reflect potential spatial variation in the relationship across different forest types; (3) a spatial linear mixed model using an NNGP with 5 neighbors; and (4) a spatial linear mixed model using an NNGP with 5 neighbors and an ecoregion-specific random slope for tree canopy cover. We ran the four candidate models for three chains of 250,000 MCMC samples discarding 190,000 samples as burn-in and using a thinning rate of 20 for a total of 9000 posterior samples. Each of the three chains was run in parallel using 5 CPU on a Linux workstation using Intel(R) Xeon(R) CPU E5-2699 v3 @ 2.30GHz with 36 CPU and 500 GB of RAM. Model run times for each chain were 2.3 hours for the non-spatial model without random slopes, 3.3 hours for the non-spatial model with random slopes, 12.9 hours for the spatial model without random slopes, and 15.4 hours for the spatial model with random slopes.

The spatially-explicit model with ecoregion-specific random slopes for tree canopy cover substantially outperformed the spatial model without random slopes ($\Delta\text{WAIC} = 1, 287$), the non-spatial model with random slopes ($\Delta\text{WAIC} = 8, 177$), and the non-spatial model without random slopes ($\Delta\text{WAIC} = 11, 390$). The top-performing model showed an overall significantly positive relationship with biomass (median = 0.54, 95% credible interval 0.43-0.66), but clear variation in the magnitude of the effect across ecoregions,

with larger magnitude values in the western US compared to the eastern US (Figure 2B main text). Biomass predictions across the US aligned with expectations, with highest biomass predicted in the Pacific Northwest (Figure 2C,D main text).

References

- Abatzoglou, J. T., Dobrowski, S. Z., Parks, S. A., and Hegewisch, K. C. (2018). TerraClimate, a high-resolution global dataset of monthly climate and climatic water balance from 1958–2015. *Scientific Data*, 5(1):1–12.
- Aguilar, O. and West, M. (2000). Bayesian dynamic factor models and portfolio allocation. *Journal of Business & Economic Statistics*, 18(3):338–357.
- Banerjee, S., Carlin, B. P., and Gelfand, A. E. (2014). *Hierarchical modeling and analysis for spatial data*. Chapman and Hall/CRC.
- Barnett, D. T., Duffy, P. A., Schimel, D. S., Krauss, R. E., Irvine, K. M., Davis, F. W., Gross, J. E., Azuaje, E. I., Thorpe, A. S., Gudex-Cross, D., et al. (2019). The terrestrial organism and biogeochemistry spatial sampling design for the National Ecological Observatory Network. *Ecosphere*, 10(2):e02540.
- Bechtold, W. A. and Patterson, P. L. (2005). *The enhanced forest inventory and analysis program—national sampling design and estimation procedures*. Number 80. USDA Forest Service, Southern Research Station.
- Coulston, J. W., Moisen, G. G., Wilson, B. T., Finco, M. V., Cohen, W. B., Brewer, C. K., et al. (2012). Modeling percent tree canopy cover: a pilot study. *Photogrammetric Engineering and Remote Sensing*, 78(7):715–727.
- Datta, A., Banerjee, S., Finley, A. O., and Gelfand, A. E. (2016). Hierarchical nearest-neighbor Gaussian process models for large geostatistical datasets. *Journal of the American Statistical Association*, 111(514):800–812.
- Dewitz, J. (2023). National Land Cover Database (NLCD) 2021 Products: U.S. Geological Survey data release. <https://doi.org/10.5066/P9JZ7A03>.
- Gelman, A. (2006). Prior distributions for variance parameters in hierarchical models (comment on article by Browne and Draper). *Bayesian Analysis*, 1(3):515–534.

- Gelman, A., Carlin, J. B., Stern, H. S., and Rubin, D. B. (2014). Bayesian data analysis (vol. 2).
- Lunn, D., Jackson, C., Best, N., Thomas, A., and Spiegelhalter, D. (2013). *The BUGS book: A Practical Introduction to Bayesian Analysis*. Chapman and Hall/CRC.
- Northrup, J. M. and Gerber, B. D. (2018). A comment on priors for Bayesian occupancy models. *PloS One*, 13(2):e0192819.
- Papastamoulis, P. and Ntzoufras, I. (2022). On the identifiability of bayesian factor analytic models. *Statistics and Computing*, 32(2):23.
- Rodenhouse, N. L. and Sillett, T. S. (2021). Valley-wide Bird Survey, Hubbard Brook Experimental Forest, 1999-2016 (ongoing). <https://doi.org/10.6073/pasta/faca2b2cf2db9d415c39b695cc7fc21>. Accessed: 2021-09-07.
- Sohl, T., Reker, R., Bouchard, M., Sayler, K., Dornbierer, J., Wika, S., Quenzer, R., and Friesz, A. (2016). Modeled historical land use and land cover for the conterminous united states. *Journal of Land Use Science*, 11(4):476–499.
- Taylor-Rodriguez, D., Finley, A. O., Datta, A., Babcock, C., Andersen, H.-E., Cook, B. D., Morton, D. C., and Banerjee, S. (2019). Spatial factor models for high-dimensional and large spatial data: An application in forest variable mapping. *Statistica Sinica*, 29:1155.
- Vecchia, A. V. (1988). Estimation and model identification for continuous spatial processes. *Journal of the Royal Statistical Society: Series B (Methodological)*, 50(2):297–312.